ELSEVIER

European Journal of Mechanics A/Solids 21 (2002) 831–843

EUROPEAN JOURNAL OF MECHANICS A/SOLIDS

Buckling and collapse of heavy tubes resting on a horizontal or inclined plane

Mark G. Blyth [a], C. Pozrikidis [b,*]

[a] *Department of Mathematics, Imperial College of Science, Technology, and Medicine, London, SW7 2BZ, UK*
[b] *Department of Mechanical and Aerospace Engineering, University of California, San Diego, La Jolla, CA 92093-0411, USA*

Received 26 November 2001; revised and accepted 14 May 2002

Abstract

The buckling and collapse of empty and liquid-filled thin-wall cylindrical tubes resting on a horizontal or inclined plane is considered. The deflection is due to the action of gravity causing the tube to deform under the influence of its own weight, or due to a negative transmural pressure pushing the tube inward on the outside. Classical thin-membrane theory is used to formulate a boundary-value problem describing the shell deformation, and the results illustrate families of deformed shapes of inextensible shells with point or segment contact occurring between the shell and the supporting surface or between two collapsed sections of the shell. The computed two-dimensional deformed shapes are used to reconstruct the three-dimensional shape of a slowly collapsing fluid-conveying vessel in the absence of significant hydrostatic pressure variations over the cross section.

Keywords: Shells; Buckling; Boundary-value problems

1. Introduction

Buckling and collapse of compliant shells is encountered in a broad variety of natural, technological, and biomedical applications including fluid transport through commercial pipelines, the wrinkling of fabric cloth, the hydroscopic buckling of paper (cockling), the waving of a flag, the floating of elastic structures and sea ice, the collapse of biological vessels under a negative transmural pressure, and the deformation of industrial capsules and biological cells enclosed by elastic membranes (Bishop et al., 1986; Bloom and Coffin, 2000; Pozrikidis, 2001).

Of particular interest are situations where the thickness of the shell is small compared to its overall size. In this limit, the elastic, plastic, and more general tangential stresses developing over the shell cross section due to deformation under load may be integrated to yield tensions or stress resultants exerted along the designated shell mid-surface. The non-uniform distribution of the tangential stresses over the cross section is responsible for the development bending moments accompanied by transverse shear tensions oriented normal to the shell surface. Equilibrium equations for forces and torques exerted over a section of the shell may then be written down in surface curvilinear or global Cartesian coordinates, and constitutive equations for the tensions and bending moments may be introduced to derive a simplified system of governing equations that are amenable to analytical and numerical methods. This approach has provided a convenient and fruitful means for assessing the stability of loaded structures and for computing stationary deformed shapes after post-buckling. In particular, small and large deformations

* Correspondence and reprints.
E-mail address: cpozrikidis@ucsd.edu (C. Pozrikidis).
URL address: http://stokes.ucsd.edu.

0997-7538/02/$ – see front matter
PII: S0997-7538(02)01235-4

Nomenclature

ρ	tube density
g	acceleration due to gravity
l	arc length
Δp_t	transmural pressure
τ, q	in-plane/shear tensions
m	bending moment
κ	curvature
κ_R	resting curvature
E_B	bending modulus
G	axial pressure gradient
Q	flow rate

of rigid and highly compliant shells have been studied extensively under the auspices of stability and bifurcation theory and in the context of boundary-value and nonlinear eigenvalue problem theory (e.g., (Antman, 1995; Libai and Simmonds, 1998; Pozrikidis, 2002a)).

In this paper, we consider the deformation of empty and liquid-filled tubular heavy shells resting on a horizontal or inclined plane. The deformation is due to the combined influence of the weight of the shell and a negative transmural pressure pushing the shell with a greater force on the outside than on the inside. Although relevant situations are familiar from everyday experience and engineering practice, our main motivation for undertaking this study has been a desire to illustrate possible modes of deformation of fluid-carrying biological vessels under general conditions.

Of particular interest to this work is the early study of Wu and Pluncett (1965) on the elastic contact between two circular shells pressed together on either side by two planar or circular surfaces of arbitrary curvature. These authors pieced together a composite solution consisting of analytical expressions for three types of segments: free segments with loads specified at the ends; segments with specified deformation; and segments with internal contact, zero tangential frictional load, and an unspecified normal load. The complementary problem of buckling and post-buckling of cylindrical shells under the action of a negative transmural pressure has been studied by a large number of authors, as will be discussed in Section 3.

The deflection of a heavy elastic shell under the influence of its own weight was first considered by Bickley (1934) for the specific purpose of developing a method for testing the mechanical properties of cotton fabric (see also (Frisch-Fay, 1962)). Much later, Wang (1981) studied the deformation of a section of a cylindrical shell with circular resting shape pinned on an inclined plane, and presented numerical solutions parameterized by the inclination angle and a dimensionless parameter involving the shell modulus of bending, the curvature of the resting configuration, and the linear density of the material. The mathematical formulation of the problem describing the equilibrium configuration of open shells, such as those studied by Wang (1981), is significantly simpler than that of the closed tubular shells presently considered, in that the order of the governing differential equation is lower by one unit.

To compute the deformed shell shapes, we work under the auspices of the generalized membrane theory for two-dimensional structures (e.g., (Steigmann and Ogden, 1997, 1999; Libai and Simmonds, 1998)). In the mathematical formulation, the tube is modeled as an inextensible elastic shell of infinitesimal thickness developing tensions and bending moments according to a linear constitutive equation when deformed from a reference configuration. A differential equation governing the distribution of the equilibrium curvature with respect to arc length is derived incorporating the effect of the body force, and solutions to a boundary-value problem are computed by numerical methods. Our interest is focused on all possible deformed shapes that constitute legitimate mathematical solutions of the governing equations with no regard to stability. In practice, nature is likely to prefer those shapes that possess minimum energy, and it is possible that only the first mode of deformation describing simple shapes will be realizable under most conditions. A rigorous mathematical discussion of the energetics and stability of higher modes would constitute further research.

The computed two-dimensional deformed shapes are used to reconstruct the three-dimensional shape of a slowly collapsing fluid-conveying, completely filled vessel when the weight of the fluid is negligible. The reconstruction procedure involves stacking together profiles at axial positions that are found by integrating the differential equation determining the axial pressure distribution in unidirectional pressure-driven flow, subject to a constant flow rate. The dimensionless coefficient relating the local pressure gradient to the flow rate is computed by solving the Poisson equation governing unidirectional viscous flow using a boundary-element method (e.g., (Pozrikidis, 1992)). High accuracy results are obtained by expressing the flow rate as a boundary integral involving the shear stress, which is available from the solution of an integral equation. In the context of

haemodynamics, such a calculation provides a relatively simple means of predicting buckling and collapse of a vein resting on surrounding tissue (Pedley, 1980). More generally, fully three-dimensional shell theory is needed to predict local collapse.

In Section 2, we present the problem statement and governing equations. In Sections 3 and 4, we discuss the results of numerical computations for weightless (unsupported) and heavy (supported) shells. In Section 5, we explain how the two-dimensional profiles of cylindrical (two-dimensional) shells may be used to construct three-dimensional shapes of fluid-carrying vessels collapsing due to an internal pressure drop that is necessary to drive the viscous flow, and present three-dimensional illustrations.

2. Problem statement and mathematical formulation

We consider the deformation of an empty or fluid-filled thin-wall cylindrical tube resting on a horizontal or inclined plane, as illustrated in Fig. 1(a). The wall of the tube consists of an elastic material that develops stresses due to the deformation from a specified reference resting state. Utilizing the generalized membrane theory (e.g., (Libai and Simmonds, 1998)), we replace the elastic stresses with tensions (stress resultants) and bending moments acting along the centerline, as illustrated in Fig. 1(b). When the plane is inclined, the shell will be assumed to be pinned at the designated origin. Our objective is to study the shape of the shell under the influence of its own weight and because of a negative transmural pressure

$$\Delta p_t \equiv p_{\text{int}} - p_{\text{ext}}, \tag{1}$$

where p_{int} is the interior pressure and p_{ext} the exterior ambient pressure.

When the tube is vacant, p_{int} is uniform along the inside surface, and the transmural pressure is constant. Under more general conditions, p_{int} may vary along the perimeter of the tube. Consider, for example, a tube that is partially filled with a stationary liquid lying underneath a gas. In this case, the interior pressure is constant along the section of the tube in contact with the gas, and increases according to the laws of hydrostatics in the direction of gravity along the section of the tube in contact with the liquid. Although our mathematical formulation allows for this possibility, for simplicity, we shall consider the fluid within the vessel to be weightless so that the transmural pressure is constant.

We begin formulating the governing equations by considering the shell in the deformed state, and identify point particles distributed along the shell by the deformed-state arc length l varying in the range $[0, L]$, where L is the shell perimeter. Because of the deformation, the shell develops an in-plane tension τ, a transverse shear tension q, and a bending moment m, as illustrated in Fig. 1(b). The vector tension exerted on a cross section of the shell is given by

$$\mathbf{T} = \tau\mathbf{t} + q\mathbf{n}, \tag{2}$$

where $\mathbf{t}$ is the unit vector tangential to the shell pointing in the direction of increasing arc length l, and $\mathbf{n}$ is the unit normal vector pointing outward.

A force balance over an infinitesimal section of the shell requires the equilibrium condition

$$\frac{\mathrm{d}\mathbf{T}}{\mathrm{d}l} + \mathbf{p} = \frac{\mathrm{d}}{\mathrm{d}l}(\tau\mathbf{t} + q\mathbf{n}) + \mathbf{p} = \mathbf{0}, \tag{3}$$

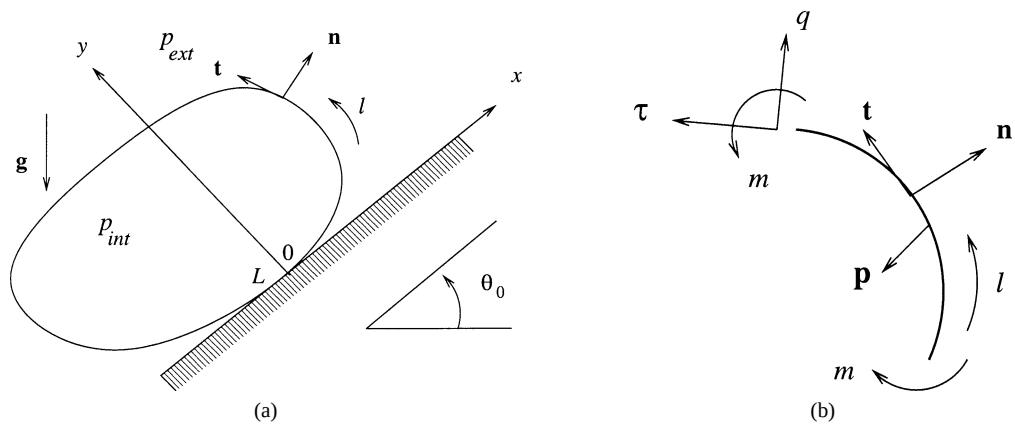

Fig. 1. (a) Illustration of a cylindrical tube resting on an inclined plane after it has deformed under the influence of its own weight or due to a negative transmural pressure. (b) Elastic tensions and bending moments developing along the wall of the tube due to the deformation.

where $\mathbf{p}$ is the distributed load due to gravity and to a non-zero transmural pressure, given by

$$\mathbf{p} = \rho\mathbf{g} + \Delta p_t \mathbf{n}, \tag{4}$$

and ρ is the constant density of the shell. In the inclined system of coordinates depicted in Fig. 1(a), the acceleration of gravity vector is given by

$$\mathbf{g} = -g\sin\theta_0 \mathbf{e}_x - g\cos\theta_0 \mathbf{e}_y, \tag{5}$$

where g is the magnitude of the acceleration of gravity, $\mathbf{e}_x$ is the unit vector along the x axis, and $\mathbf{e}_y$ is the unit vector along the y axis.

Expanding out the derivatives of the products in (3) and using the relations

$$\frac{\mathrm{d}\mathbf{t}}{\mathrm{d}l} + \kappa\mathbf{n} = \mathbf{0}, \qquad \frac{\mathrm{d}\mathbf{n}}{\mathrm{d}l} - \kappa\mathbf{t} = \mathbf{0}, \qquad \kappa = \frac{\mathrm{d}\alpha}{\mathrm{d}l}, \tag{6}$$

where κ is the curvature of the shell in the xy plane and α is the angle subtended between the tangent $\mathbf{t}$ and the x-axis, we obtain the normal and tangential scalar force balances

$$-\kappa\tau + \frac{\mathrm{d}q}{\mathrm{d}l} = -\mathbf{p}\cdot\mathbf{n} \equiv -p_n, \qquad \kappa q + \frac{\mathrm{d}\tau}{\mathrm{d}l} = -\mathbf{p}\cdot\mathbf{t} \equiv -p_t. \tag{7}$$

The tangential and normal components of the load are given by

$$p_t = \rho\mathbf{g}\cdot\mathbf{t}, \qquad p_n = \rho\mathbf{g}\cdot\mathbf{n} + \Delta p_t, \tag{8}$$

where, according to our earlier discussion, the transmural pressure Δp_t can be allowed to be a function of arc length. Solving the first of Eqs. (7) for τ and substituting the result into the second equation, we derive a second-order differential equation governing the distribution of the transverse shear tension,

$$\frac{\mathrm{d}}{\mathrm{d}l}\left[\frac{1}{\kappa}\left(\frac{\mathrm{d}q}{\mathrm{d}l} + p_n\right)\right] + \kappa q + p_t = 0. \tag{9}$$

Performing next a moment balance over an infinitesimal section of the shell, we find

$$q = \frac{\mathrm{d}m}{\mathrm{d}l}. \tag{10}$$

At this stage, we introduce a constitutive equation for the bending moments expressed by the linear relation

$$m = E_B(\kappa - \kappa_R), \tag{11}$$

where E_B is the bending modulus, and $\kappa_R(l)$ is the curvature of the shell in a resting configuration where the bending moments are assumed to vanish (e.g., (Steigmann and Ogden, 1997, 1999; Pozrikidis, 2002a)). The theory of thin plates provides us with the estimate $E_B = Eh^3/[12(1-\nu^2)]$, where E is the volume modulus of elasticity, ν the Poisson ratio, and h the shell thickness (e.g., (Fung, 1965, p. 461)). Heretoforth, we shall assume that h and thus E_B is constant, independent of position along the shell mid-plane.

Substituting (11) into (10) and using the resulting expression to eliminate q from (9), we obtain a differential equation governing the distribution of the curvature,

$$\frac{\mathrm{d}}{\mathrm{d}l}\left[\frac{1}{\kappa}\left(\frac{\mathrm{d}^2(\kappa-\kappa_R)}{\mathrm{d}l^2} + \frac{p_n}{E_B}\right)\right] + \kappa\frac{\mathrm{d}(\kappa-\kappa_R)}{\mathrm{d}l} + \frac{p_t}{\kappa_b} = 0, \tag{12}$$

which can be recast into the form:

$$\frac{\mathrm{d}}{\mathrm{d}l}\left[\frac{1}{\kappa}\left(\frac{\mathrm{d}^2(\kappa-\kappa_R)}{\mathrm{d}l^2} + \frac{p_n}{E_B} + \frac{1}{2}\kappa^3\right)\right] - \kappa\frac{\mathrm{d}\kappa_R}{\mathrm{d}l} + \frac{p_t}{E_B} = 0. \tag{13}$$

Integrating (13) once with respect to l, we derive the integro–differential equation

$$\frac{\mathrm{d}^2\kappa}{\mathrm{d}l^2} = -\frac{1}{2}\kappa(\kappa^2 + c) - \frac{p_n}{E_B} + \frac{\mathrm{d}^2\kappa_R}{\mathrm{d}l^2} + \kappa\int_{l_0}^{l}\kappa(l')\frac{\mathrm{d}\kappa_R}{\mathrm{d}l'}\mathrm{d}l' - \frac{\rho}{E_B}\mathbf{g}\cdot\big[\mathbf{x}(l) - \mathbf{x}(l_0)\big], \tag{14}$$

where c is an integration constant with dimensions of inverse squared length, and l_0 is an arbitrarily specified arc length. Substituting (5) into (4) and the result into (14), we derive the more explicit form:

$$\frac{\mathrm{d}^2\kappa}{\mathrm{d}l^2} = -\frac{1}{2}\kappa(\kappa^2+c) - \frac{\Delta p_t}{E_B} - \frac{\rho g}{E_B}\left[\cos\theta_0\frac{\mathrm{d}x}{\mathrm{d}l} - \sin\theta_0\frac{\mathrm{d}y}{\mathrm{d}l}\right] + \frac{\mathrm{d}^2\kappa_R}{\mathrm{d}l^2} + \kappa\int_{l_0}^{l}\kappa(l')\frac{\mathrm{d}\kappa_R}{\mathrm{d}l'}\mathrm{d}l'$$
$$+ \frac{\rho g}{E_B}\kappa\big\{\sin\theta_0\big[x(l)-x(l_0)\big] + \cos\theta_0\big[y(l)-y(l_0)\big]\big\}. \tag{15}$$

Note that the derivative of the resting curvature, but not the curvature itself, appears in the equilibrium equation (15). Furthermore, the Cartesian coordinates and their derivatives with respect to arc length appear only when the gravitational term is present.

It is important to emphasize that a constitutive equation for the in-plane tension τ may be additionally imposed, and its role will be to determine the total length of the shell in the deformed state, L, and the relative distribution of point particles along the deformed contour with respect to the resting configuration. Thus, shell inextensibility is required only insofar as to provide justification for the constitutive equation for the bending moments with uniform shell thickness, as discussed in the end of the paragraph following Eq. (11). On a practical level, inextensibility is invoked to define the *a priori* unknown reference curvature distribution $\kappa_R(l)$, where l is the arc length around the shell in the *deformed* state; an exception occurs when κ_R is constant, as in the case of a circular unstressed shell or a rolled-up flat sheet.

The boundary conditions accompanying (15) depend on the particular problem under consideration. For example, symmetry conditions may be imposed to capture shapes with a desired set of symmetries. In all cases, Eq. (15) involves an unspecified constant c that may play the role of an eigenvalue. Multiple solutions corresponding to bifurcating or disconnected solution branches are possible, as will be discussed in Section 3.

At small and moderate deformations, a heavy shell resting on a horizontal or inclined plane touches the support at a single point where the shell is locally concave upward and turns away from the plane, as depicted in Fig. 2(a). As the shell becomes increasingly deformed, the curvature at the contact point is reduced, and the shell tends to spread over the support. At critical conditions, the contact-point curvature vanishes and a transition occurs from single-point contact to contact over a finite segment. The end-points of the segment are unknown in advance and must be found as part of the solution from the requirement of vanishing curvature. A similar behavior occurs when two remote sections of a weightless or heavy shell collapse and are pressed together, as illustrated in Fig. 2(b).

Consider a weightless shell that has collapsed onto itself to form two loops, as illustrated in Fig. 2(b). Requiring that the total force exerted on each one of the two loops on either side of the contact point or segment vanish, we find that the in-plane tension at the contact point must vanish. Setting τ in the first of Eqs. (7) equal to zero, and using (9), (10) and (11) with $\rho = 0$, we derive a boundary condition for the curvature at the contact point in terms of the constant c. For example, in the case of a shell with uniform resting curvature, we find

$$\kappa^2 = -c. \tag{16}$$

which plays the role of a mixed boundary condition.

Nondimensionalizing all lengths and distances using the total perimeter of the shell in the deformed state, L, we find that the shape of the shell is determined by three parameters: the inclination angle θ_0, the dimensionless transmural pressure

$$\Delta\hat{p} \equiv -\frac{\Delta p_t}{E_B\kappa_u^3}, \tag{17}$$

and the dimensionless density of the shell material

$$\hat{\rho} \equiv \frac{\rho g}{E_B\kappa_u^3}. \tag{18}$$

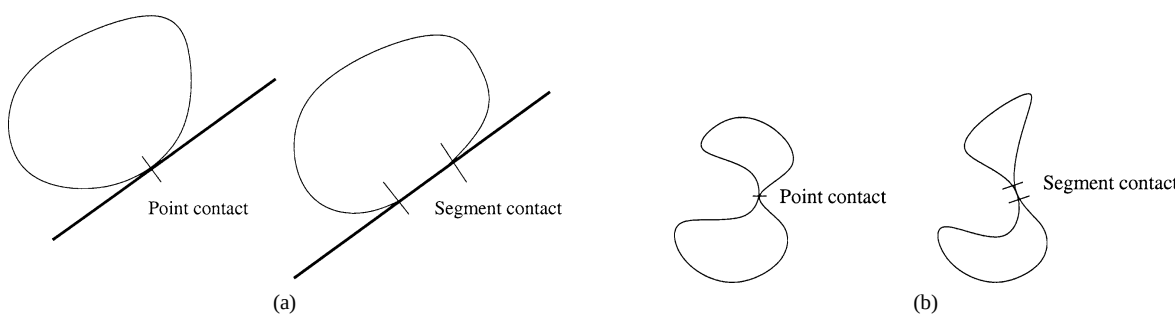

Fig. 2. Pointwise and segment contact of (a) a shell resting on an inclined plane, and (b) two remote sections of a collapsed shell.

The constant $\kappa_u = 2\pi/L$ is the equivalent curvature of an inextensible shell that is circular in the undeformed state. Note that a positive dimensionless transmural pressure corresponds to negative physical transmural pressure causing collapse.

The boundary value problem described in this section was solved using a shooting method, where improvements were made using Newton's method. The differential equation itself was solved using the fourth-order Runge–Kutta method, and parameter continuation was employed to describe solutions that belong to the same branch.

3. Weightless shells

Significant simplifications occur when the density of the shell is negligible, corresponding to $\hat{\rho} = 0$. In this limit, the supporting presence of the inclined plane is not required. Previous numerical and asymptotic studies have revealed the existence of multiple solution branches when the dimensionless transmural pressure $\Delta\hat{p}$ exceeds a sequence of thresholds that depend on the undeformed resting shape. In the case of shells with circular resting shapes, buckled shapes are possible for all values of $\Delta\hat{p} \geqslant 3$, whereas in the case of shells with non-circular resting states, the undeformed shape is immediately modified upon the imposition of a negative transmural pressure, however small (e.g., (Pozrikidis, 2002a)).

3.1. Circular shells

Consider first shells with circular undeformed shapes and uniform resting curvature κ_R. In this case, all but the first two terms on the right-hand side of (15) drop out, leaving a simplified expression. A perturbation analysis shows that small deformations from the circular state are possible when $\Delta\hat{p} = n^2 - 1$, for any integer $n > 1$ (e.g., (Pozrikidis, 2002a)). Solution branches emanating from these critical points describing buckled shapes with n-fold rotational symmetry were computed by several previous authors using numerical methods (Tadjbakhsh, 1969; Flaherty et al., 1972; Pozrikidis, 2002a).

The numerical results of Flaherty et al. (1972) revealed that, as a solution branch is traversed in the direction of increasing $\Delta\hat{p}$, the severity of the shell deformation increases until, eventually, a critical value $\Delta\hat{p}_c$ is reached where point contact and subsequent unphysical self-intersection takes place. A second solution branch describing non-penetrating shapes with point contact arises as the pressure difference is raised beyond $\Delta\hat{p}_c$ until a further critical value, $\Delta\hat{p}_o$. Beyond the second critical value, for $\Delta\hat{p} > \Delta\hat{p}_o$, the contact points spread over contact segments whose length increases with $\Delta\hat{p}$, while the shell assumes self-similar shapes.

By way of testing our numerical method and simultaneously verifying the previous results, we have recomputed the deformed shapes and the critical pressures identified by previous authors. Sample results are shown in Fig. 3. In the numerical computations, periodic and symmetry boundary conditions are imposed for post-buckled shapes with no points of contact, and condition (16) is imposed for shapes with point contact. When point contact occurs with $n \geqslant 2$, we require

$$0 \leqslant l \leqslant l_1: \qquad \kappa'(0) = 0, \qquad \kappa^2(l_1) = -c, \qquad \int_0^{l_1} \kappa(\xi)\,\mathrm{d}\xi = \frac{\pi}{2}, \tag{19}$$

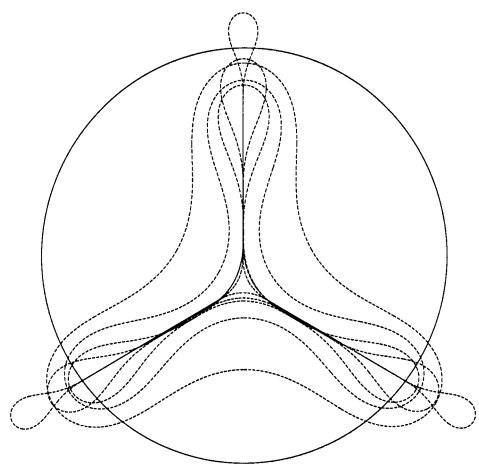

Fig. 3. Buckled shapes with three-fold symmetry ($n = 3$) (dotted lines) for a shell with a circular resting state (solid line).

Table 1
Computed values of the critical transmural contact pressures for modes $n = 2, 3, 4$

	$\Delta\hat{p}_c$			$\Delta\hat{p}_o$		
$n \rightarrow$	2	3	4	2	3	4
FKR	5.247	21.65	51.84	10.34	81.81	207.2
Present	5.246	21.65	51.84	10.33	81.80	207.2

Here, as elsewhere, the subscripts c and o represent the point and segment contact critical values, respectively. "FKR" indicates figures given by Flaherty et al. (1972).

$$l_1 \leqslant l \leqslant \frac{L}{2n}: \qquad \kappa^2(l_1) = -c, \qquad \kappa'\left(\frac{L}{2n}\right) = 0, \qquad \int_{l_1}^{L/(2n)} \kappa(\xi)\,\mathrm{d}\xi = \frac{L}{2n} - \frac{\pi}{2}, \tag{20}$$

where the origin of arc length has been set at the lowest point of the shapes shown in Fig. 3, and l_1 is the arc length at the first point of contact. Except in the special case $n = 2$ where $l_1 = L/4$, the unspecified length l_1, must be computed as part of the solution. Our computed values of the critical pressures are in good agreement with those given by Flaherty et al. (1972), as shown in Table 1.

3.2. Non-circular shells

Consider now shells with non-uniform resting curvature described by the model equation

$$\kappa_R(l) = \bar{\kappa} + \kappa' \cos(\kappa_u s l), \tag{21}$$

where s is a natural number, $\bar{\kappa}$ is the arc-length averaged curvature, and the coefficient κ' expresses the amplitude of the resting curvature. It is convenient to introduce the intermediate function $g(l)$, defined by

$$\frac{\mathrm{d}g}{\mathrm{d}l} = \kappa \frac{\mathrm{d}\kappa_R}{\mathrm{d}l}, \tag{22}$$

which is to be solved together with a modified version of (14) with the integral term replaced by g and the constant c set to zero. The solution was computed by a shooting method where the unknown initial value $g(0)$ is found as part of the solution.

Pozrikidis (2002a) presented bifurcation diagrams illustrated possible solution branches for varying $\Delta\hat{p}$ when $s = 2$ and $s = 3$. To facilitate our discussion, these diagrams are reproduced with the solid lines in Fig. 4. The vertical axis is the curvature at the lowest point reduced by the reference curvature $\kappa_u = 2\pi/L$, where L is the total arc length of the shell. In both cases, $s = 2, 3$, the shell deforms as soon as the transmural pressure becomes negative. This contrasts with situations encountered in Section 3.1 where the pre-buckled solution with uniform curvature is apparently valid for all values of $\Delta\hat{p}$, although it is of course highly unlikely that this shape is stable. Pozrikidis (2002a) computed solutions up to and beyond the point where the shells self-intersect. As an extension of the earlier work, we here allow for the development of points and lines of contact. By way of demonstrating the possible configurations, we will discuss solutions for the cases $s = 2$ with $\kappa'/\kappa_u = 0.25$.

Following the upper branch marked 1 in Fig. 4(a), we find that the deformed shapes develop a dimple of increasing amplitude until point of contact appears at the critical pressure difference $\Delta\hat{p}_c = 4.70$. The shapes found by traversing branch 2 develop in a similar but not identical manner, now reaching single-point contact at the critical value $\Delta\hat{p}_c = 5.78$. Little deformation occurs following branch 3, and the shell deviates only slightly from its incipient elliptical-like profile. Solution branches labeled 4 and 5 describe shapes with three-fold rotational symmetry. Critical shapes with three points of contact occur at the value $\Delta\hat{p}_c = 20.81$, calculated accurate to four significant figures, on both branches. The comparable values reflect the near symmetry of branches 4 and 5 apparent in the bifurcation diagram 4(a).

To illustrate the shapes of deformed shells with non-uniform resting curvature beyond the critical point of contact, we trace the shapes occurring along branch 1 in Fig. 4(a), corresponding to $s = 2$. In practice, these shapes are likely to represent the most stable configurations, at least for long tubes where the deviation from two-dimensionality is small. In the numerical computation, the boundary conditions at the point of contact are adjusted in a manner similar to that discussed earlier for the circular unstressed shapes. The length l_1 is kept as an unknown and is subsequently found to have the expected value $L/4$ to within the precision of the calculation. The results show that shapes with point contact occur in the range $4.70 < \Delta\hat{p} < 10.03$; whereafter, a line of contact develops. The dotted line in Fig. 4(a) shows the corresponding solution branch emanating from the critical pressure $\Delta\hat{p}_c = 4.70$.

It is not possible to find self-similar shapes with line contact, as it is possible for shells with circular resting shapes, and the numerical calculation must be done in full for every value of $\Delta\hat{p}$. For shapes with segment contact, the calculation is performed over the range $0 \leqslant l \leqslant l_1$, subject to the boundary conditions

$$\kappa'(0) = 0, \qquad \kappa(l_1) = 0, \qquad \theta(0) = 0, \qquad \theta(l_1) = \pi/2, \qquad g(l_1) = 0. \tag{23}$$

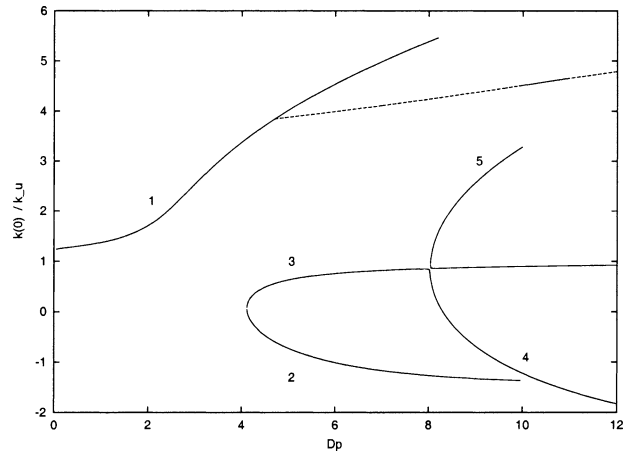

(a)

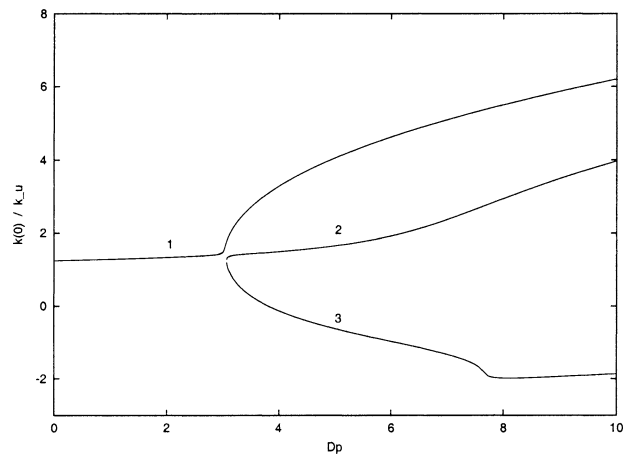

(b)

Fig. 4. Bifurcation diagrams showing the solution spaces for (a) an elliptical-like resting shape, $s = 2$, and (b) $s = 3$. The dotted line in (a) traces a branch corresponding to shells with point and line contact.

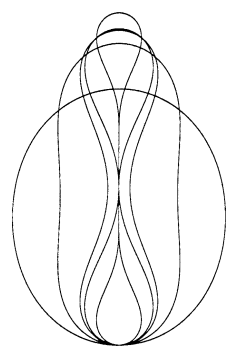

Fig. 5. Shell shapes computed at various points along the branch labeled 1 in Fig. 4(a). From left to right, $\Delta\hat{p} = 1.0,\ 2.86,\ 4.22,\ 6.0,\ 25.0$.

The remaining portion, $l_1 \leqslant l \leqslant L/4$, is completed with a straight segment of an appropriate length. Figure 5 illustrates a family of computed solutions with no contact, point contact, and segment contact.

We computed corresponding shapes for mode $s = 3$ and $\kappa'/\kappa_u = 0.25$, and found that the shell develops a single point of contact along the upper branch labeled 1 at the critical pressure $\Delta\hat{p}_c = 5.23$. The shapes corresponding to branch 2 of Fig. 4(b)

develop a trio of contact points at the critical pressure $\Delta\hat{p}_c = 20.51$. The shapes along branch 3 are similar to those along branch 1, eventually establishing a single point of contact when $\Delta\hat{p}_c = 5.33$.

4. Heavy shells

In Section 3, we discussed the buckled states of weightless shells corresponding to $\hat{\rho} = 0$. We now turn to examining configurations of heavy shells resting on a horizontal or inclined plane, taking also into account the effect of a non-zero transmural pressure. The equilibrium shape of the shell is described by Eq. (15) accompanied by suitable boundary conditions. Because the x and y coordinates and their derivatives with respect to arc length appear explicitly in this equation, we must introduce, and simultaneously solve for, the nonlinear equations

$$\frac{\mathrm{d}x_1}{\mathrm{d}l} = x_3, \qquad \frac{\mathrm{d}x_2}{\mathrm{d}l} = x_4, \qquad \frac{\mathrm{d}x_3}{\mathrm{d}l} = -\kappa x_4, \qquad \frac{\mathrm{d}x_4}{\mathrm{d}l} = \kappa x_3, \tag{24}$$

where $x = x_1(l)$, $y = x_2(l)$, $x' = x_3$, $y' = x_4$, and a prime denotes a derivative with respect to the independent variable, l. Using elementary differential geometry, we find that the curvature is given by the expressions $\kappa = -x_1''x_2' + x_1'x_2'' = -x_1''/x_2' = x_2''/x_1'$, which allows us to relate the curvature to the shell shape. For a shell pinned to the surface at $x = y = 0$, the initial conditions follow as $x_1(0) = 0$, $y_1(0) = 0$, $x_3(0) = 1$ and $x_4(0) = 0$.

When the dimensionless density and transmural pressure are sufficiently small, we expect that the shell will have a single point of contact at the origin. Furthermore, by analogy with the case of weightless shells, we anticipate that point contact will persist until critical conditions, whereupon the shell will tend to penetrate the supporting surface. Continuing the calculation beyond this value will still produce shapes with physical significance, representing shells sagging down on either side of a single point of support. Our main interest, however, lies in permitting the development of a line of contact between the shell and the surface to imitate a heavy elastic membrane resting on a plane. Thus, at the critical conditions where the curvature at the point of contact vanishes, the boundary conditions are adapted to accommodate this behavior. Further changes in the nature of the contact between the shell and the wall, or indeed itself, must also be accompanied by suitable changes in the boundary conditions. Recall that, once the curvature is known, the transverse shear tension $q(l)$ may be found using (9) and (10). The in-plane tension τ may then be computed in a straightforward manner using the first equation in (5).

First, we discuss shells resting on a horizontal plane, $\theta_0 = 0$, for $\Delta\hat{p} = 0$. For small values of $\hat{\rho}$, self-contact does not occur, the governing differential equations are integrated all the way around the shell, and suitable conditions are imposed at $l = 0$, $L/2$, and $l = L$. To begin with, we assume a circular resting shape and seek solutions that are symmetric with respect to the y-axis that is normal to the plane, by requiring

$$\kappa'(0) = 0, \qquad \kappa'\left(\frac{L}{2}\right) = 0, \qquad \int_0^{L/2} \kappa(\xi)\,\mathrm{d}\xi = \pi, \qquad x(L) = 0. \tag{25}$$

Note that the curvature at the point of contact is *a priori* unknown. Line contact between the shell and the supporting surface occurs at the critical value $\hat{\rho} = \hat{\rho}_{c1}$ where $\kappa(0) = 0$. To describe shapes with a line of contact along the base, we replace the first of conditions (25) with $\kappa(l_1) = 0$, where the unspecified length l_1 marking the location of the end-point of the line of contact is found as part of the solution. Continuing the calculations for increasing values of $\hat{\rho} > \hat{\rho}_{c1}$, we find that the top of the shell begins to droop down in the middle, eventually making contact with the base at the origin at the second critical value $\hat{\rho} = \hat{\rho}_{c2}$. The boundary conditions are then adapted to account for this new point of contact, and the calculations continue to higher values of $\hat{\rho} > \hat{\rho}_{c2}$.

Typical shell shapes corresponding to vanishing transmural pressure are shown in Fig. 6. The numerical results reveal that the critical dimensionless densities where spreading over the plane and self-contact occur are given by $\hat{\rho}_{c1} = 0.593$ and $\hat{\rho}_{c2} = 5.679$. At the upper point of contact developing when $\hat{\rho} > \hat{\rho}_{c2}$, the curvature is negative. As the dimensionless density $\hat{\rho}$ is raised, the top curvature increases in magnitude in a monotonic fashion, ultimately passing through zero at the critical value $\hat{\rho} = \hat{\rho}_{c3} = 11.878$. For higher densities, the dimpled point of contact at the origin spreads out to form a new line along the interior side of the base. Once again, the boundary conditions are amended by the introduction of a further unknown l_2 representing the half-length of the new contact line, and the computations continue for values $\hat{\rho} > \hat{\rho}_{c3}$.

Next, we consider the effect of the dimensionless transmural pressure $\Delta\hat{p}$. One might reasonably expect that a negative $\Delta\hat{p}$ with a sufficiently large magnitude will tend to restore the resting shape assumed in the absence of gravity, and further increase will eventually lead to the likely rupture of the shell due to large elastic tensions, although our equations do not incorporate the necessary physics to predict this breakdown. By contrast, a positive dimensionless transmural pressure will deflate the shell still further, accentuating the flattening trend apparent in Fig. 6. Figure 7(a) demonstrates the effect of the transmural pressure on the curvature at the lowest point for various dimensionless densities $\hat{\rho}$, for shell with point contact. Figure 7(b) shows the

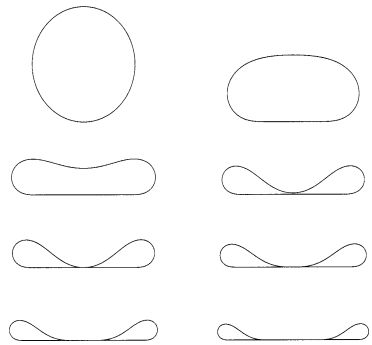

Fig. 6. Shapes of a heavy elastic shell with a circular resting shape sitting on a horizontal surface ($\theta_0 = 0$) for $\hat{\rho} = 0.0$, 1.61, 4.29, 5.64, 6.05, 11.88, 17.91, 36.28, spanning each of the four regimes discussed in the text.

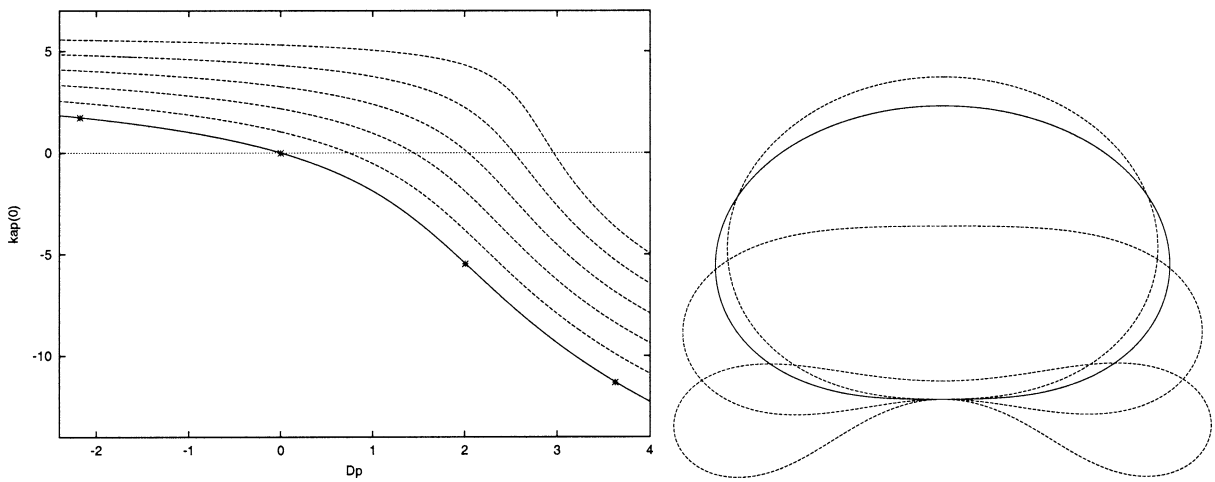

(a) (b)

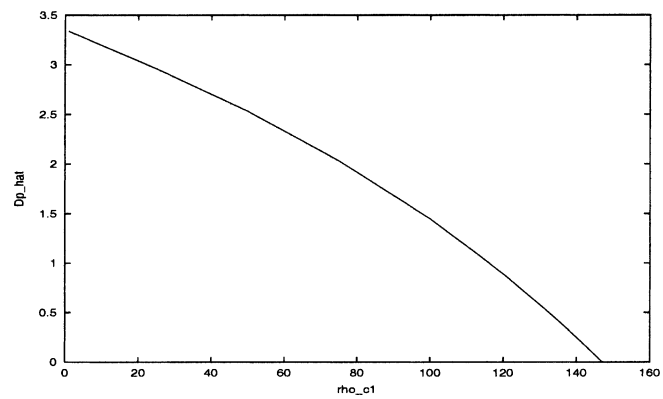

(c)

Fig. 7. Effect of the transmural pressure on a heavy shell with a circular resting shape. (a) Curvature at the lowest point, $\kappa(0)$ plotted against $\Delta\hat{p}$ for $\hat{\rho} = \hat{\rho}_{c1} = 0.593$ (solid line), and 0.504, 0.404, 0.303, 0.202 and 0.101 from left to right (dotted lines). (b) Shell shapes corresponding to values of $\Delta\hat{p}$ marked on the solid line in (a) in an obvious physical manner; the base state ($\Delta\hat{p} = 0$) is plotted with a solid line. (c) Dependence of the critical value $\hat{\rho}_{c1}$ on the transmural pressure.

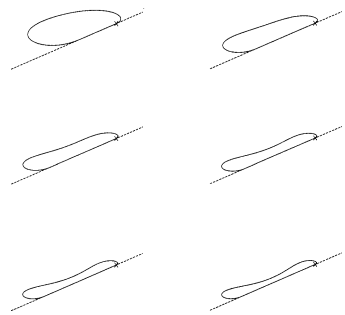

Fig. 8. Heavy elastic shells sitting on a plane inclined at an angle $\theta_0 = \pi/4$, for dimensionless density $\hat{\rho} = 0.81$, 2.41, 4.03, 5.64, 6.85 and 8.06. The crosses indicate the points where the shells are pinned to the plane.

shell profiles for a fixed value of $\hat{\rho}$ corresponding to the marked points on the lowest curve in Fig. 7(a). The effect of $\Delta\hat{p}$ on the first critical density $\hat{\rho}_{c1}$ where the shell spreads over the wall is illustrated in Fig. 7(b). Note that $\Delta\hat{p} = 3.34$ when $\hat{\rho}_{c1} = 0$, in agreement with the value computed by Pozrikidis (2002a) for a weightless buckled shell with a circular resting shape.

We proceed next to consider the buckling of shells resting on an inclined plane, held stationary by a pinning force. With θ_0 non-zero, it is now necessary to solve the full equation (15) with all terms retained on the right-hand side. Once again, we set l_0=0 and $x(l_0) = y(l_0) = 0$, and choose the boundary conditions at each deformation mode as in the case of the horizontal plane. The results are qualitatively similar: for small enough values of $\hat{\rho}$, the shells rest with a single point of contact on the inclined plane; as $\hat{\rho}$ is sufficiently increased, the shapes begin to intersect the plane. For zero transmural pressure, the transition occurs when $\hat{\rho} = \hat{\rho}_{c1} = 0.2729$ whereupon the curvature vanishes at the contact point. We have calculated shapes beyond the critical value $\hat{\rho}_{c1}$ up to about $\hat{\rho} = 8$. Much beyond this value, the time required for each calculation becomes prohibitively expensive. Fig. 8 displays some of the computed shapes for the representative case $\theta_0 = \pi/4$. Note that the shells begin to droop down slowly in the middle, and a second point of contact is ultimately established at a second critical value of $\hat{\rho}$.

5. Flow through a collapsing tube

Consider now steady pressure-driven viscous flow through a collapsing tube whose cross-section changes slowly in the axial direction z, so that the flow may be considered to be locally unidirectional. Subject to this approximation, the axial component of the velocity, u_z, satisfies the parametrically forced Poisson equation

$$\nabla^2 u_z = -\frac{G(z)}{\mu}, \tag{26}$$

where $\nabla^2 \equiv \partial^2/\partial x^2 + \partial^2/\partial y^2$ is the Laplacian operator over the tube cross section, $G(z) \equiv -\partial p_{\text{int}}/\partial z$ is the negative of the pressure gradient in the streamwise direction inside the tube, and μ is the fluid viscosity. The no-slip boundary condition requires that u_z vanish around the tube contour in the xy plane.

It is convenient to express the flow rate through the tube in the form:

$$Q \equiv \int u_z \,\mathrm{d}x\,\mathrm{d}y = \delta(z)\frac{G\pi a^4}{8\mu}, \tag{27}$$

where the integral is computed over the tube cross section, δ is the dimensionless hydraulic conductivity determined by the tube cross sectional shape, $a = L/(2\pi)$ is the equivalent tube radius, and L is the tube perimeter. In the case of a circular tube, a is the tube radius and Poiseuille's law requires $\delta = 1$ (e.g., (Pozrikidis, 1997)). Our previous discussion suggests that the tube contour, and thus δ, is a function of the density of the shell and transmural pressure.

Rearranging (27), using the definition of G, assuming that the external pressure is constant and the internal pressure is uniform over the cross section, thereby neglecting hydrostatic pressure variations, we derive an ordinary differential equation for Δp,

$$\mathrm{d}z = \frac{\pi a^4}{8\mu Q}\delta(z)\,\mathrm{d}\Delta p_t, \tag{28}$$

which may be recast into the dimensionless form:

$$\mathrm{d}\hat{z} = \delta(\hat{z})\,\mathrm{d}\Delta\hat{p}, \tag{29}$$

where $\hat{z} \equiv z\widehat{Q}/a$ is the reduced axial position, and $\widehat{Q} \equiv 8\mu Q/(\pi E_B)$ is a dimensionless flow rate. Assuming that an initially circular tube starts collapsing at $z = z_0$ where $\Delta\hat{p} = n^2 - 1$, for integer n, we may integrate Eq. (29) to generate the function $\Delta\hat{p}(\hat{z})$ and its inverse. Once this has been accomplished, the three-dimensional shape of a collapsing tube may be reconstructed by stacking next to one another adjacent cross sections, spacing them by the appropriate distances.

We have reformulated the Poisson equation (26) as an integral equation for the boundary distribution of the shear stress, and then solved it using a boundary-element method (e.g., (Pozrikidis, 2002b)). The numerical procedure involves decomposing the axial velocity u_z into a particular solution that satisfies the Poisson equation with a constant right-hand side and a homogeneous component that satisfies Laplace's equation, and then solving for the boundary distribution of the normal derivative of the homogeneous solution. The end-points of the boundary elements are generated by solving the boundary-value problem described in previous sections. Once the boundary distribution of the normal derivative is available, the flow rate Q and coefficient δ are computed by evaluating a boundary integral (Pozrikidis, 2002a). Testing showed that discretization into 128 uniform straight elements is sufficient for obtaining δ accurate to the third significant figure.

The solid line in Fig. 9(a) shows a graph of the dimensionless hydraulic conductivity δ plotted against $\Delta\hat{p}$ for the shapes displayed in Fig. 3. The line terminates at the point where opposite sections of the tube come into point contact at a critical

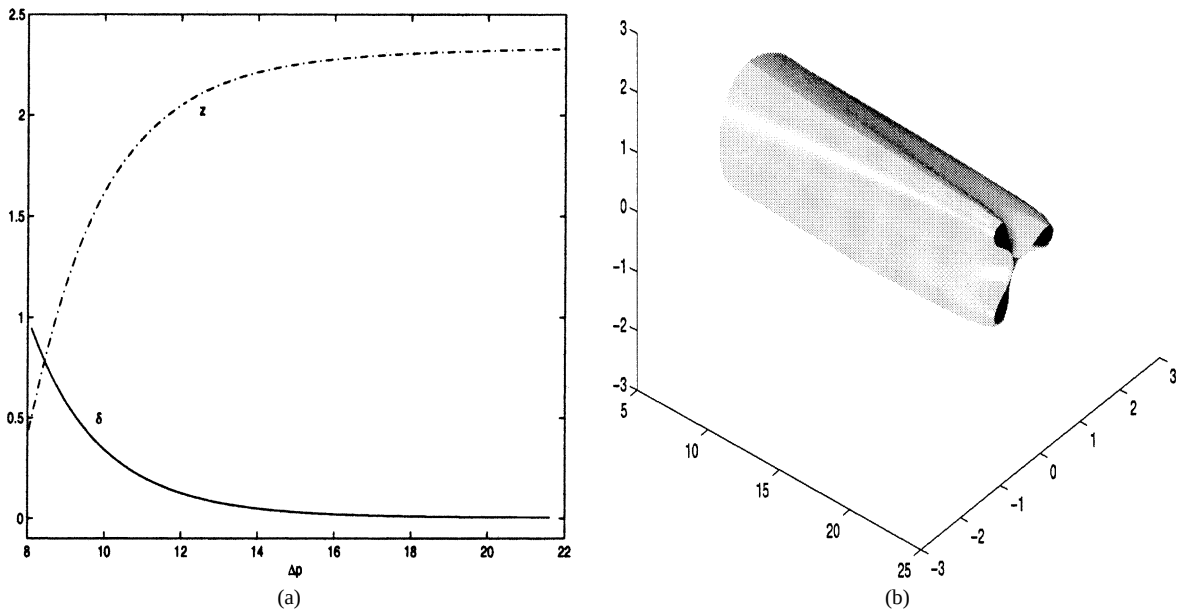

Fig. 9. Flow in a buckled tube with three-fold symmetry up to the point of contact. (a) Dependence of the downstream location $\hat{z}$ and hydraulic conductivity δ on the transmural pressure $\Delta\hat{p}$. (b) The buckling tube.

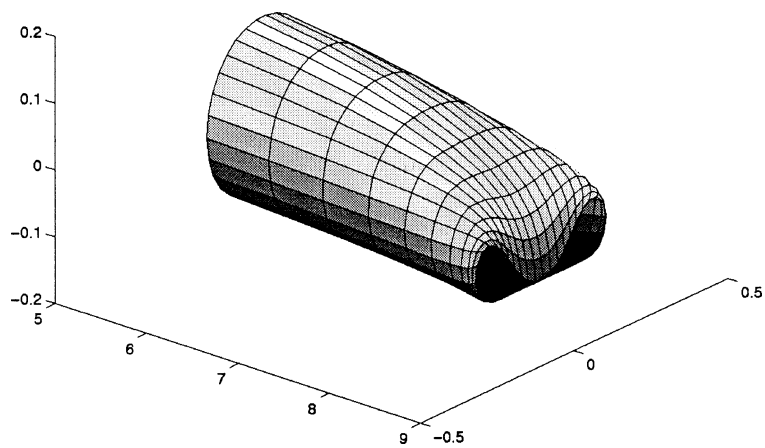

Fig. 10. Flow in a heavy collapsible tube resting of a horizontal plane for $\hat{\rho} = 140.0$.

transmural pressure, as illustrated in the bifurcation diagram displayed in Fig. 4(b). The dashed line shows the corresponding axial position $\hat{z}$ generated by integrating Eq. (29) using a numerical method. These results were used to reconstruct the three-dimensional shape of a tube collapsing in the $n = 3$ mode in terms of two-dimensional cross sections, as discussed in the paragraph after Eq. (29), and the result is shown in Fig. 9(b).

Figure 10 shows the result of a similar calculation for flow in a heavy collapsible tube resting on a horizontal plane for $\hat{\rho} = 140.0$, up to the point where the top of the tube makes contact with the base.

6. Discussion

We have discussed the mathematical formulation and presented numerical solutions of the equations governing the shape of a light or heavy tubular shell resting on a horizontal or inclined plane. The problem formulation accounts for the effects of gravity on the tube wall and for a negative transmural pressure. The numerical results extend the work of previous authors in several ways; most importantly with respect to the significance of non-circular resting shapes, especially after self-contact, and to the effect of the shell weight. Shapes with wall-shell point and segment contact and multiple contact were found under conditions of extreme deformation.

We have computed the three-dimensional shapes of fluid-conveying tubes collapsing slowly due to a decrease in the internal pressure with streamwise distance. In practice, three-dimensional tubes are clamped at one or both ends or meet other tubes at junctions and bifurcations, which are known to have an important effect of the prevailing modes of deflection (e.g., (Yamaki, 1984)). For example, the three-fold deflection mode is preferred near the end of a clamped tube. To describe the shapes of such shells, a fully three-dimensional calculation is necessary. The development of numerical methods for this purpose is the subject of current research.

References

Antman, S.S., 1995. Nonlinear Problems of Elasticity. Springer-Verlag, New York.

Bickley, W.G., 1934. The heavy elastica. Philos. Mag. Ser. 7 (17), 603–622.

Bishop, R.E.D., Price, W.G., Wu, Y., 1986. A general linear hydroelasticity theory of floating structures moving in a seaway. Philos. Trans. Roy. Soc. London Ser. A 316, 375–426.

Bloom, F., Coffin, D., 2000. Handbook of Thin Plate Buckling and Postbuckling. Chapman & Hall. CRC, Boca Raton, FL.

Flaherty, J.E., Keller, J.B., Rubinow, S.I., 1972. Post-buckling behavior of elastic tubes and rings with opposite sides in contact. SIAM J. Appl. Math. 23, 446–455.

Frisch-Fay, R., 1962. Flexible Bars. Butterworths, London.

Fung, Y.C., 1965. Foundations of Solid Mechanics. Prentice Hall International, Englewood Cliffs, NJ.

Libai, I., Simmonds, J.G., 1998. The Nonlinear Theory of Elastic Shells. Cambridge University Press, New York.

Pedley, T.J., 1980. The Fluid Mechanics of Large Blood Vessels. Cambridge University Press, Cambridge.

Pozrikidis, C., 1992. Boundary Integral and Singularity Methods for Linearized Viscous Flow. Cambridge University Press, New York.

Pozrikidis, C., 1997. Introduction to Theoretical and Computational Fluid Dynamics. Oxford University Press, New York.

Pozrikidis, C., 2001. Effect of bending stiffness of the deformation of capsules in simple shear flow. J. Fluid Mech. 440, 269–291.

Pozrikidis, C., 2002a. Buckling and collapse of open and closed cylindrical shells. J. Engrg. Math. 42, 157–180.

Pozrikidis, C., 2002b. A Practical Guide to Boundary Element Methods with the Software Library BEMLIB. Chapman & Hall. CRC, Boca Raton, FL.

Steigmann, D.J., Ogden, R.W., 1997. Plane deformations of elastic solids with intrinsic boundary elasticity. Proc. Roy. Soc. London Ser. A 453, 853–877.

Steigmann, D.J., Ogden, R.W., 1999. Elastic surface-substrate interactions. Proc. Roy. Soc. London Ser. A 455, 427–474.

Tadjbakhsh, T., 1969. Buckled states of elastic rings. In: Keller, J.B., Antman, S. (Eds.), Bifurcation Theory and Nonlinear Eigenvalue Problems. Benjamin, New York, pp. 69–92.

Wang, C.Y., 1981. Equilibrium of a heavy, naturally curved sheet on an inclined plane. Z. Angew. Math. Mech. 61, 267–269.

Wu, C.-H., Plunkett, R., 1965. On the contact problem of thin circular rings. J. Appl. Meth. 11, 11–20.

Yamaki, N., 1984. Elastic Stability of Circular Cylindrical Shells. North-Holland, Amsterdam.